PHYSICAL REVIEW A VOLUME 22, NUMBER 1 JULY 1980

Monte Carlo calculation of the Born-Oppenheimer potential between two helium atoms

R. E. Lowther and R. L. Coldwell
Department of Physics, University of Florida, Gainesville, Florida 32611
(Received 16 March 1979; revised manuscript received 20 March 1980)

Fully correlated Hylleraas-type electronic wave functions and a biased-selection Monte Carlo method have been used to find a rigorous upper bound to the Born-Oppenheimer potential between two helium atoms. The potential agrees with the experimental results of Burgmans, Farrar, and Lee (BFL) to within 1.4 Monte Carlo standard deviations for all nuclear separation distances calculated (4.5–15.0a_B). At the potential minimum of 5.6a_B this bound (-7.10 ± 0.30 Ry) is slightly below the BFL value of -6.70 Ry.

INTRODUCTION

The importance and extremely small size of the well depth has made the ground-state helium-helium pair potential the subject of much theoretical and experimental attention with estimates of this depth ranging from −9.1 to −13.5 K. The recent experimental curves begin with Bruch and McGee,[1] who in 1970 fitted a pair potential with a well depth of −10.75 K to dilute-gas properties. Also in 1970, Bennewitz *et al.*[2] found a well depth of −10.4 K from total scattering cross-section measurements. Differential-scattering cross-section measurements were made in 1973 by Farrar and Lee,[3] who found a well depth of -11.0 ± 0.2 K. Burgmans, Farrar, and Lee[4] (hereafter BFL) in 1976 revised this experiment, obtaining a depth of −10.57 K. Nuclear-spin relaxation in dilute gases has also been recognized as a sensitive means of studying intermolecular forces. Chapman[5] in 1975 performed measurements of this on dilute helium gas, finding a potential of the Bruch-McGee form but with a deeper well depth of −11.5 K.

The theoretical work begins in 1931 with a paper by Slater and Kirkwood,[6] who found a helium-helium potential (depth = −9.1 K) by joining a repulsive energy term, which worked well for small internuclear separations, with an attractive dipole-dipole interaction which they could calculate at large distances. Margenau,[7] also in 1931, extended this formalism to include dipole-quadrupole and quadrupole-quadrupole interactions. This lowered the curve to a depth of -13.5 ± 1.5 K, with the quadrupole-quadrupole term accounting for only 3% of the depth at the minimum. Configuration-interaction (CI) calculations were carried out from 1970–1972 by McLaughlin and Schaefer[8] (−12.0 K), Bertoncini and Wahl[9] (−12.0 K), and others. Attempts to correct or account for the neglect of a large (200–2000 times the size of the well depth) part of the intra-atomic correlation energy missed by these calculations were done by Liu and McLean[10] (−11.0 K), Bertoncini and Wahl[11] (−10.8 K), Dacre[12] (−10.54 K), and Burton[13] (−10.55 K). A good discussion of the problem this correlation energy poses to CI calculations is given in Ref. 10. A calculation (1976) using perturbation theory was carried out by Chalasinski and Jeziorski,[14] who found a lower "bound" of −13.4 K. When they approximately corrected for intra-atomic correlation effects, an upper bound of −10.7 K was obtained.

When the integrals are done by the Monte Carlo method, any form for the wave function satisfying the boundary conditions is integrable. This makes it possible to construct wave functions by appropriately piecing together extremely accurate atomic wave functions[15] found in the literature accounting for all (to within 5.0×10^{-9} Ry) of the intra-atomic correlation energy. Since it is not necessary to subtract the infinite nuclear separation energy to find the energy at another nucleus-nucleus distance, these energies are variational upper bounds. It is also possible to put explicitly into the wave functions the attractive multipole terms of the Slater-Kirkwood formalism.[6,7]

This work is a refinement of an earlier work,[16] with the main differences being an improved form for the wave function and more Monte Carlo points evaluated to give answers precise enough to generate a curve. The method of picking these points, the minimization technique, and the method used to obtain energy differences between two nuclear separation distances is exactly the same, however, and is explained similarly (including proofs for the various biased selection theorems) in the earlier paper.

WAVE FUNCTION

Following Slater,[6] we start with atomic wave functions for nucleus A at $\vec{R}_A$ and nucleus B at $\vec{R}_B$, with spin-up electrons at $\vec{r}_1$ and $\vec{r}_2$ and spin-down electrons at $\vec{r}_3$ and $\vec{r}_4$, and write the trial wave function as

$$\Psi(\vec{r}_1,\vec{r}_2,\vec{r}_3,\vec{r}_4)=(1-P_{12}-P_{34}+P_{12}P_{34})\psi_A(\vec{r}_1,\vec{r}_3)\times\psi_B(\vec{r}_2,\vec{r}_4)\exp[-\tfrac{1}{2}U(\vec{r}_1,\vec{r}_3;\vec{r}_2,\vec{r}_4)]\,. \tag{1}$$

P_{ij} is the permutation operator between parallel electrons i and j. The term $\psi_A(\vec{r}_1,\vec{r}_3)$ is Schwartz's[15] 189-term Hylleraas-type atomic wave function (Table I) for electrons 1 and 3 on nucleus A. The function U, which accounts for interactions for electrons near nucleus A with those near nucleus B, contains terms similar to Slater's dipole-dipole term,[6] and can be written as

$$U(\vec{r}_1,\vec{r}_3;\vec{r}_2,\vec{r}_4)=u(\vec{r}_1;\vec{r}_2)+u(\vec{r}_1;\vec{r}_4)+u(\vec{r}_3;\vec{r}_2)+u(\vec{r}_3;\vec{r}_4)\,, \tag{2}$$

where

$$u(\vec{r}_i;\vec{r}_j)=\sum_{\nu=0}^{3}V_\nu(\vec{r}_i;\vec{r}_j)+e(\vec{r}_i;\vec{r}_j)\,. \tag{3}$$

The term V_0 is very similar to the interaction potential energy

$$V_0(\vec{r}_i;\vec{r}_j)=[(R_{AB}^2+\alpha)^{-1/2}-(r_{iB}^2+\alpha)^{-1/2}-(r_{jA}^2+\alpha)^{-1/2}+(r_{ij}^2+\alpha)^{-1/2}]f_0(r_{iA})f_0(r_{jB})\,, \tag{4}$$

with $R_{AB}=|\vec{R}_A-\vec{R}_B|$ and $\vec{r}_{iA}=|\vec{r}_i-\vec{R}_A|$, etc. The variable parameter α, given in Table II, was introduced to eliminate the singularities in this term. The term V_1 is the dipole-dipole term given as

$$V_1(\vec{r}_i;\vec{r}_j)=(x_{iA}x_{jB}+y_{iA}y_{jB}-2z_{iA}z_{jB})f_1(r_{iA})f_1(r_{jB})\,, \tag{5}$$

with x_{iA}, y_{iA}, etc. the x,y,z components of $\vec{r}_{iA}$.

TABLE I. Parameters c_{lmn} reading from left to right in Schwartz's 189-term atomic wave function $\sum_{l,m,n}c_{lmn}s^l u^m t^n e^{-1.75s}$. The "integers" (l,m,n) are in the order: (0,0,0); (1,0,0), (0,1,0); $(\frac{3}{2},0,0)$, $(\frac{1}{2},1,0)$; (2,0,0), (1,1,0), (0,2,0), (0,0,2); $(\frac{5}{2},0,0)$, $(\frac{3}{2},1,0)$, $(\frac{1}{2},2,0)$, $(\frac{1}{2},0,2)$; etc. Note s includes half-integer powers while t includes even powers only.

1.000 000 000	$-5.676\,206\,449\times10^{-1}$	$6.388\,872\,059\times10^{-1}$	3.601 649 402	$-2.018\,472\,944$
$-1.902\,943\,036\times10^{+1}$	$1.244\,899\,486\times10^{+1}$	$-1.026\,802\,958$	$7.632\,663\,324\times10^{-1}$	$6.422\,960\,944\times10^{+1}$
$-4.603\,636\,465\times10^{+1}$	$3.361\,217\,000$	$-3.069\,398\,340$	$-1.469\,536\,530\times10^{+2}$	$1.121\,025\,918\times10^{+2}$
$-1.037\,848\,041\times10^{+1}$	$1.306\,100\,183\times10^{+1}$	3.436 179 707	$-4.799\,940\,197$	$2.399\,759\,883\times10^{+2}$
$-1.923\,960\,173\times10^{+2}$	$2.770\,135\,115\times10^{+1}$	$-3.904\,835\,778\times10^{+1}$	$-1.695\,078\,037\times10^{+1}$	$2.374\,837\,556\times10^{+1}$
$-2.885\,316\,167\times10^{+2}$	$2.414\,376\,047\times10^{+2}$	$-5.531\,899\,045\times10^{+1}$	$8.110\,744\,231\times10^{+1}$	$4.525\,372\,476\times10^{+1}$
$-6.698\,419\,033\times10^{+1}$	$-2.913\,505\,181$	6.129 375 841	$1.724\,980\,398\times10^{-1}$	$2.599\,999\,412\times10^{+2}$
$-2.260\,694\,210\times10^{+2}$	$7.999\,811\,368\times10^{+1}$	$-1.205\,385\,629\times10^{+2}$	$-7.982\,978\,682\times10^{+1}$	$1.267\,617\,020\times10^{+2}$
$1.215\,969\,591\times10^{+1}$	$-2.579\,764\,611\times10^{+1}$	$-8.255\,664\,738\times10^{-1}$	$-1.770\,633\,923\times10^{+2}$	$1.594\,372\,166\times10^{+2}$
$-8.394\,132\,610\times10^{+1}$	$1.305\,978\,447\times10^{+2}$	$9.848\,670\,095\times10^{+1}$	$-1.677\,336\,023\times10^{+2}$	$-2.439\,385\,675\times10^{+1}$
$5.303\,597\,090\times10^{+1}$	1.445 389 874	$7.006\,484\,610\times10^{-1}$	$-1.951\,982\,372$	$2.799\,597\,276\times10^{-1}$
$9.116\,479\,191\times10^{+1}$	$-8.473\,931\,080\times10^{+1}$	$6.420\,011\,583\times10^{+1}$	$-1.038\,851\,622\times10^{+2}$	$-8.683\,079\,074\times10^{+1}$
$1.578\,020\,986\times10^{+2}$	$3.004\,298\,892\times10^{+1}$	$-6.738\,126\,236\times10^{+1}$	$-1.252\,469\,963$	$-2.213\,914\,998$
6.162 512 424	$-8.210\,878\,221\times10^{-1}$	$-3.521\,437\,808\times10^{+1}$	$3.366\,445\,734\times10^{+1}$	$-3.572\,976\,454\times10^{+1}$
$6.047\,768\,002\times10^{+1}$	$5.498\,596\,657\times10^{+1}$	$-1.059\,388\,848\times10^{+2}$	$-2.452\,697\,604\times10^{+1}$	$5.679\,962\,058\times10^{+1}$
$4.703\,998\,025\times10^{-1}$	3.120 412 013	$-8.754\,168\,625$	1.199 648 526	$-4.621\,098\,536\times10^{-2}$
$1.724\,975\,592\times10^{-1}$	$-8.879\,909\,237\times10^{-2}$	$-7.212\,391\,498\times10^{-4}$	$1.002\,670\,936\times10^{+1}$	$-9.812\,668\,097$
$1.429\,921\,553\times10^{+1}$	$-2.540\,266\,224\times10^{+1}$	$-2.479\,212\,340\times10^{+1}$	$5.029\,554\,086\times10^{+1}$	$1.356\,885\,188\times10^{+1}$
$-3.238\,420\,030\times10^{+1}$	$8.716\,991\,675\times10^{-2}$	$-2.511\,910\,999$	7.138 739 963	$-1.066\,658\,882$
$9.943\,179\,167\times10^{-2}$	$-3.692\,937\,706\times10^{-1}$	$1.858\,350\,881\times10^{-1}$	$1.921\,603\,082\times10^{-3}$	$-2.038\,107\,176$
2.029 710 542	$-4.005\,407\,440$	7.476 147 452	7.758 764 735	$-1.646\,348\,439\times10^{+1}$
$-5.036\,841\,074$	$1.235\,055\,282\times10^{+1}$	$-1.721\,607\,346\times10^{-1}$	1.234 795 512	$-3.562\,579\,879$
$5.948\,614\,116\times10^{-1}$	$-8.737\,071\,941\times10^{-2}$	$3.245\,351\,907\times10^{-1}$	$-1.647\,217\,345\times10^{-1}$	$-1.118\,357\,309\times10^{-3}$
$7.315\,085\,265\times10^{-4}$	$-3.836\,780\,819\times10^{-3}$	$4.364\,745\,962\times10^{-3}$	$-8.215\,236\,068\times10^{-4}$	$2.793\,244\,470\times10^{-1}$
$-2.808\,997\,643\times10^{-1}$	$7.448\,460\,687\times10^{-1}$	$-1.459\,459\,700$	$-1.599\,800\,986$	3.528 033 111
1.201 623 207	$-3.016\,330\,989$	$7.635\,602\,081\times10^{-2}$	$-3.677\,896\,122\times10^{-1}$	1.077 487 048
$-2.022\,013\,328\times10^{-1}$	$3.895\,799\,143\times10^{-2}$	$-1.452\,645\,159\times10^{-1}$	$7.594\,162\,605\times10^{-2}$	$-1.824\,394\,960\times10^{-5}$
$-8.971\,180\,790\times10^{-4}$	$4.675\,354\,267\times10^{-3}$	$-5.237\,388\,480\times10^{-3}$	$9.668\,982\,706\times10^{-4}$	$-2.308\,777\,869\times10^{-2}$
$2.321\,560\,230\times10^{-2}$	$-8.254\,948\,939\times10^{-2}$	$1.693\,984\,877\times10^{-1}$	$1.951\,928\,160\times10^{-1}$	$-4.446\,743\,096\times10^{-1}$
$-1.664\,063\,669\times10^{-1}$	$4.260\,428\,116\times10^{-1}$	$-1.566\,465\,228\times10^{-2}$	$6.109\,913\,795\times10^{-2}$	$-1.815\,735\,190\times10^{-1}$
$3.817\,256\,327\times10^{-2}$	$-8.768\,071\,553\times10^{-3}$	$3.288\,568\,040\times10^{-2}$	$-1.793\,108\,591\times10^{-2}$	$1.665\,615\,371\times10^{-4}$
$3.695\,103\,522\times10^{-4}$	$-1.916\,123\,574\times10^{-3}$	$2.154\,616\,496\times10^{-3}$	$-4.103\,343\,655\times10^{-4}$	$-1.651\,409\,751\times10^{-6}$
$1.303\,109\,147\times10^{-5}$	$-3.168\,170\,870\times10^{-5}$	$1.789\,193\,139\times10^{-5}$	$-3.132\,109\,060\times10^{-7}$	$8.678\,468\,784\times10^{-4}$
$-8.616\,083\,210\times10^{-4}$	$4.124\,028\,815\times10^{-3}$	$-8.832\,131\,764\times10^{-3}$	$-1.066\,184\,506\times10^{-2}$	$2.494\,894\,907\times10^{-2}$
$1.015\,980\,123\times10^{-2}$	$-2.643\,277\,259\times10^{-2}$	$1.276\,404\,132\times10^{-3}$	$-4.347\,994\,712\times10^{-3}$	$1.308\,412\,679\times10^{-2}$
$-3.060\,459\,698\times10^{-3}$	$7.933\,139\,599\times10^{-4}$	$-2.994\,343\,269\times10^{-3}$	$1.714\,345\,730\times10^{-3}$	$-3.347\,126\,314\times10^{-5}$
$-5.101\,264\,671\times10^{-5}$	$2.634\,949\,065\times10^{-4}$	$-3.016\,779\,448\times10^{-4}$	$6.119\,936\,532\times10^{-5}$	$6.474\,281\,604\times10^{-7}$
$-5.047\,403\,976\times10^{-6}$	$1.208\,128\,981\times10^{-5}$	$-6.751\,485\,425\times10^{-6}$	$1.161\,691\,551\times10^{-7}$	

The nuclei are located on the z axis. Similarly, the dipole-quadrupole (V_2) term is given as

$$V_2(\vec{r}_i;\vec{r}_j)=[r_{iA}^2 z_{jB}-r_{jB}^2 z_{iA}+(z_{iA}-z_{jB})(2x_{iA}x_{jB}+2y_{iA}y_{jB}-3z_{iA}z_{jB})]f_2(r_{iA})f_2(r_{jB})\,. \tag{6}$$

The quadrupole-quadrupole term (V_3) is

$$\begin{aligned}V_3(\vec{r}_{iA};\vec{r}_{jB})=\{&6\vec{r}_{iA}\cdot\vec{r}_{jB}[\vec{r}_{iA}\cdot\vec{r}_{jB}-r_{iA}^2-r_{jB}^2+5(z_{iA}-z_{jB})^2]-15(z_{iA}^2r_{jB}^2+z_{jB}^2r_{iA}^2)\\&+z_{iA}z_{jB}[30(r_{iA}^2+r_{jB}^2)-70(z_{iA}^2+z_{jB}^2)+105z_{iA}z_{jB}]+3r_{iA}^2r_{jB}^2\}f_3(r_{iA})f_3(r_{jB})\,.\end{aligned} \tag{7}$$

The functions f_ν are splines of the form

$$f(r)=\sum_{i=1}^{6}a_i(\xi_i-r)_+^3, \tag{8}$$

where

$$(x)_+=\begin{cases}x\,, & x>0\\ 0\,, & x<0\,.\end{cases} \tag{9}$$

The functions f_ν therefore become zero for large values of their arguments and thereby tend to make the V_ν terms a function of the interactions of the electrons near atom A with those near atom B. Finally, to allow for close encounters of electrons not already accounted for by the atomic wave functions, the term

$$e(\vec{r}_i;\vec{r}_j)=e(r_{ij})=\sum_{i=1}^{2}a_i'(\xi_i'-r_{ij})_+^3, \tag{10}$$

with the cusp condition $e'(0)=-1$, was added. The coefficients a_i, a_i' and knots ξ_i', given in Table II, are parameters with respect to which the trial wave functions were optimized. The knots ξ_i were kept fixed at 2.0, 4.0, 6.0, 7.0, 8.0, and $9.0a_B$. This wave function includes many more terms than that of Ref. 16. In addition, the factor $e^{-U/2}$ is now operated on by the permutation operators, and $U(\vec{r}_1,\vec{r}_3;\vec{r}_2,\vec{r}_4)$, which was completely symmetric in Ref. 16, now contains only inter-

TABLE II. Variable parameters for Eqs. (4), (8), and (10) which, together with Schwartz's parameters, determine the wave functions.

R	4.5	5.0	5.6	6.6	7.5	9.0	15.0
α	1.0000×10^{-1}	1.0000×10^{-1}	3.9924×10^{-1}	4.0000×10^{-1}	3.9803×10^{-1}	3.9987×10^{-1}	3.9835×10^{-1}
V_0	-4.7089×10^{-2}	-1.5583×10^{-2}	-4.2959×10^{-4}	7.4717×10^{-3}	-4.2037×10^{-2}	-6.1447×10^{-2}	-6.4346×10^{-3}
coefs	4.1521×10^{-2}	2.2278×10^{-2}	-1.0755×10^{-2}	1.0305×10^{-2}	6.3929×10^{-2}	1.7560×10^{-1}	2.0789×10^{-2}
	5.4473×10^{-2}	7.8756×10^{-2}	1.6640×10^{-1}	9.0902×10^{-2}	-7.2103×10^{-3}	-3.2004×10^{-1}	1.2476×10^{-1}
	-2.7733×10^{-1}	-3.2257×10^{-1}	-4.3716×10^{-1}	-3.9917×10^{-1}	-3.0104×10^{-1}	1.7480×10^{-2}	-5.0135×10^{-1}
	3.1603×10^{-1}	3.5785×10^{-1}	4.2082×10^{-1}	4.5883×10^{-1}	4.2732×10^{-1}	3.3921×10^{-1}	5.6004×10^{-1}
	-1.1112×10^{-1}	-1.2501×10^{-1}	-1.3856×10^{-1}	-1.6297×10^{-1}	-1.6199×10^{-1}	-1.6693×10^{-1}	-1.9667×10^{-1}
V_1	-4.0905×10^{-3}	-1.2673×10^{-3}	-2.9824×10^{-5}	8.2965×10^{-4}	2.0435×10^{-4}	7.5887×10^{-4}	
coefs	4.4357×10^{-3}	2.0280×10^{-3}	-7.1245×10^{-4}	7.1370×10^{-4}	1.8854×10^{-3}	-3.5555×10^{-3}	
	6.3760×10^{-3}	7.9808×10^{-3}	1.2760×10^{-2}	4.9998×10^{-3}	2.6079×10^{-4}	5.9674×10^{-3}	
	-3.0702×10^{-2}	-3.1495×10^{-2}	-3.4104×10^{-2}	-2.1873×10^{-2}	-1.0598×10^{-2}	1.2614×10^{-3}	
	3.4495×10^{-2}	3.4546×10^{-2}	3.3041×10^{-2}	2.5188×10^{-2}	1.4426×10^{-2}	-8.5693×10^{-3}	
	-1.2057×10^{-2}	-1.2011×10^{-2}	-1.0910×10^{-2}	-8.9565×10^{-3}	-5.4013×10^{-3}	3.9646×10^{-3}	
V_2	-2.4806×10^{-3}	-5.5842×10^{-4}	-1.2493×10^{-5}	2.4690×10^{-4}	-6.1789×10^{-4}	2.5186×10^{-4}	
coefs	2.1474×10^{-3}	9.2387×10^{-4}	-2.4570×10^{-4}	3.8712×10^{-4}	6.2379×10^{-4}	-7.1978×10^{-4}	
	1.7942×10^{-3}	2.4902×10^{-3}	4.7003×10^{-3}	1.1790×10^{-3}	7.8279×10^{-5}	1.3118×10^{-3}	
	-1.0797×10^{-2}	-1.1683×10^{-2}	-1.2755×10^{-2}	-7.6704×10^{-3}	-2.9010×10^{-3}	-7.1619×10^{-5}	
	1.2454×10^{-2}	1.3361×10^{-2}	1.2428×10^{-2}	9.6142×10^{-3}	3.9015×10^{-3}	-1.3904×10^{-3}	
	-4.3854×10^{-3}	-4.7208×10^{-3}	-4.1135×10^{-3}	-3.5272×10^{-3}	-1.4532×10^{-3}	6.8425×10^{-4}	
V_3	-5.6161×10^{-4}	-7.6796×10^{-5}	-1.5489×10^{-6}	-1.4792×10^{-5}	-4.3603×10^{-4}		
coefs	2.7491×10^{-4}	7.6504×10^{-5}	-5.9322×10^{-6}	-4.8355×10^{-5}	1.0740×10^{-3}		
	2.2679×10^{-4}	2.7861×10^{-4}	4.3438×10^{-4}	-6.5031×10^{-5}	-3.3810×10^{-4}		
	-1.3134×10^{-3}	-1.2744×10^{-3}	-1.2774×10^{-3}	6.8490×10^{-4}	-3.7789×10^{-3}		
	1.5016×10^{-3}	1.4496×10^{-3}	1.2796×10^{-3}	-9.0871×10^{-4}	5.5581×10^{-3}		
	-5.2679×10^{-4}	-5.1116×10^{-4}	-4.2849×10^{-4}	3.3956×10^{-4}	-2.1221×10^{-3}		
E-E	-2.8192	$1.3295\times10^{+1}$	4.9865×10^{-1}	-3.0147	-3.2710	-1.9430	-1.9627
coefs	3.2066	-8.0949×10^{-1}	-1.0998	2.3911	1.8616	1.1371	1.1371
E-E	1.1376	2.6041×10^{-1}	1.2589	9.3485×10^{-1}	5.0101×10^{-1}	8.2637×10^{-1}	8.2220×10^{-1}
knots	1.1143	8.3781×10^{-1}	6.4453×10^{-1}	1.1141	7.8747×10^{-1}	1.2083	1.2083

actions between electrons on the left of the semicolon with those on the right. This allowed the functions f to be longer ranged so that $f(r_{3B})$ could overlap appreciably with $f(r_{1A})$ without interfering with the already accurate atomic wave function $\psi_A(\vec{r}_1, \vec{r}_3)$.

MONTE CARLO METHOD

Exactly as in Ref. 16, the 12-dimensional Monte Carlo points $\tilde{x}_i$, which contain the coordinates of the electrons, were picked with an average probability w_i. This results in the introduction of w_i into the sums to correct for this bias, resulting in

$$E_{Nt} = \frac{\sum_{i=1}^{N} \Psi_t(\tilde{x}_i) H \Psi_t(\tilde{x}_i)/w_i}{\sum_{i=1}^{N} \Psi_t^2(\tilde{x}_i)/w_i} \tag{11}$$

for the expectation value of H with the wave function Ψ_t. One sum was taken with $N = 377\,000$ for the internuclear distances 4.5, 5.0, and $5.6a_B$ and the corresponding differences. Another was taken over an independent set of points with $N = 782\,000$ for the internuclear distances $5.6-15.0a_B$.

As is shown in Ref. 17, the standard deviation in E_{Nt} is given by

$$\sigma_{Nt}^2 = \frac{\sum_{i=1}^{N} [\Psi_t(\tilde{x}_i) H \Psi_t(\tilde{x}_i) - E_{Nt} \Psi_t^2(\tilde{x}_i)]^2/w_i^2}{[\sum_{i=1}^{N} \Psi_t^2(\tilde{x}_i)/w_i]^2} . \tag{12}$$

This is easily seen to be zero when $H\Psi_t(\tilde{x}_i) = E_{Nt}\Psi_t(\tilde{x}_i)$ for all values of $\tilde{x}_i$.

An electron position in the point $\tilde{x}_i$ had probabilities of being picked in the different ways:

(a) With respect to nucleus A (or B). In this case the distances $r_{kA} = |\vec{r}_{kA}|$ was chosen with a constant probability for small distances (introducing a $1/r_{kA}^2$ into w_i) and for larger distances with probability r_{kA}^2 times the square of the Hartree-Fock atomic wave function (introducing the square of the Hartree-Fock atomic wave function into w_i).

(b) With respect to any previously picked electron position $\vec{r}_j$. In this case the distance $r_{kj} = |\vec{r}_k - \vec{r}_j|$ was chosen with probability r_{kj} (introducing a $1/r_{kj}$ into w_i).

(c) With respect to a point midway between the nuclei.

(d) With respect to a huge box centered on the nuclei.

The final w_i for the point $\tilde{x}_i$ is an average over all possible ways of having picked this point. This includes averaging over permutations of parallel-spin electrons. The averaging technique is rigorous and is explained in the Appendix of Ref. 16. Note that if any of the interparticle distances r are small, then the resulting $1/r$ or $1/r^2$ in w_i will dominate all other terms, causing w_i to be proportional to this term. This decreases the importance of such terms in Eqs. (11) and (12). It accomplishes this, of course, by greatly increasing the probability of finding such points. This weighting is exactly that needed to remove the singularities in the potential part of H.

Using the scaling technique described in Ref. 16, differences between energies at different nuclear separations also were calculated. These differences (along with the corresponding standard deviations) and the values from Eqs. (11) and (12) are given in Table III.

The wave functions were optimized by minimizing σ^2 and not the energy (see Ref. 17). The minimization of σ^2 Eq. (12) with respect to the parameters in Ψ_t was as follows. A small number n of the Monte Carlo points $\tilde{x}_i$ was selected, then one ($\tilde{x}_p$) was chosen from these with a probability equal to

$$p = \frac{[\Psi_t^2(\tilde{x}_p)/w_p]^{1/2}}{\sum_{i=1}^{n} [\Psi_t^2(\tilde{x}_i)/w_i]^{1/2}} . \tag{13}$$

This, of course, introduces a new w to be used in calculating σ^2 and to a certain extent brings back the singularities eliminated above. 1000 such points were found using $n = 2$. For each point the fixed values of the atomic wave functions and their first and second derivatives were stored.

TABLE III. Energies, energy differences, and kinetic energies with standard deviations in units of 10^{-5} Ry.

R_i	$E(R_i)$	$E(R_i) - E(R_{i+1})$	$E(R_i) - E(R_{i+2})$	$K(R_i) - K(15)$
4.5	41.35 ± 1.29	41.19 ± 0.68	48.52 ± 0.93	643 ± 25
5.0	0.16 ± 0.82	7.33 ± 0.34		216 ± 19
5.6	−7.16 ± 0.33	−2.92 ± 0.22	−5.01 ± 0.24	61 ± 16
6.6	−4.24 ± 0.29	−2.09 ± 0.13	−3.43 ± 0.16	19 ± 14
7.5	−2.15 ± 0.25	−1.34 ± 0.07	−1.99 ± 0.13	17 ± 12
9.0	−0.81 ± 0.22	−0.65 ± 0.07		15 ± 9
15.0	−0.16 ± 0.21			

This enabled the standard deviation of a trial wave function to be calculated extremely rapidly over these 1000 points. The simplex method[18] was then used to find the parameter set minimizing σ^2.

CURVE FIT

The values from Eqs. (11) and (12) and these differences—most of which are given in Table III—were used in a curve fit minimizing

$$\chi^2=\sum_{i=1}^{7}\left(\frac{E_{\rm fit}(R_i)-E_{\rm MC}(R_i)}{\lambda_i\sigma_{\rm MC}(R_i)}\right)^2 + \sum_{i=1}^{15}\left(\frac{\Delta E_{\rm fit}(R_i,(\Delta R)_i)-\Delta E_{\rm MC}(R_i,(\Delta R)_i)}{\hat{\lambda}_i\hat{\sigma}_{\rm MC}(R_i,(\Delta R)_i)}\right)^2, \quad (14)$$

where

$$\Delta E(R_i,(\Delta R)_i)=E(R_i+(\Delta R)_i)-E(R_i), \quad (15)$$

and $\hat{\sigma}_{\rm MC}(R_i,(\Delta R)_i)$ is the Monte Carlo standard deviation of $\Delta E_{\rm MC}(R_i,(\Delta R)_i)$. The factors λ_i and $\hat{\lambda}_i$ made it possible to test for the relative importance of these terms. The best final result had error bars about 3% less than would have been found with $\lambda_i=\hat{\lambda}_i=1.0$. This yields

$$E_{\rm fit}(R)=E_{\rm BFL}(R)+\sum_{i=1}^{5}c_i(R-4.0)_+^2(k_i-R)_+^2, \quad (16)$$

with $\{c_i\}=+0.558\,029\times10^{-5}$, $-0.592\,108\times10^{-6}$, $-0.140\,675\times10^{-6}$, $-0.349\,129\times10^{-7}$, $-0.709\,027\times10^{-9}$ Ry/a_B^4, and $\{k_i\}=5.6$, 6.6, 7.5, 9.0, and $15.0a_B$. The term $E_{\rm BFL}(R)$ is the experimental curve of Burgmans, Farrar, and Lee[4] which was used because it goes to the accepted[19] limits at small ($R<4.0a_B$) and large ($R>10.0a_B$) internuclear distances. $E_{\rm fit}(R)$ and $E_{\rm BFL}(R)$ for $5.0a_B<R<9.5a_B$ are given in Table IV and Fig. 1.

The Monte Carlo standard deviation in the fit can be found by squaring the equation

$$E_N-E_\infty=-\sum_{i=1}^{N}\delta_i \quad (17)$$

and taking an ensemble average. E_∞ is the true ($N=\infty$) energy for Ψ_i and δ_i is the error introduced into E_N by omitting the ith point. This yields the formula for the standard deviation of the energy $E_N=E_N(R)$ at nuclear separation distance R on the curve:

$$\langle(E_N-E_\infty)^2\rangle=\left\langle\sum_{i=1}^{N}\sum_{j=1}^{N}\delta_i\delta_j\right\rangle=\left\langle\sum_{i=1}^{N}\delta_i^2\right\rangle\approx\sum_{i=1}^{N}\delta_i^2. \quad (18)$$

Our estimate for this quantity (Table IV) was found by breaking our total run into 1159 partial runs, each representing a point i, and redoing the curve fit successively leaving each of these out.

TABLE IV. Energies with standard deviations from the curve fit along with the experimental results of Burgmans, Farrar, and Lee in units of 10^{-5} Ry.

R	$E_{\rm BFL}$	$E_{\rm MC}$
5.0	0.36	0.26 ± 0.52
5.1	−2.35	−2.51 ± 0.48
5.2	−4.22	−4.44 ± 0.43
5.3	−5.44	−5.73 ± 0.38
5.4	−6.18	−6.53 ± 0.34
5.5	−6.57	−6.96 ± 0.31
5.6	−6.70	−7.10 ± 0.30
5.7	−6.65	−7.04 ± 0.29
5.8	−6.48	−6.87 ± 0.28
5.9	−6.23	−6.61 ± 0.27
6.0	−5.93	−6.30 ± 0.26
6.1	−5.60	−5.94 ± 0.25
6.2	−5.25	−5.57 ± 0.24
6.3	−4.90	−5.20 ± 0.23
6.4	−4.54	−4.82 ± 0.22
6.5	−4.20	−4.46 ± 0.21
6.6	−3.88	−4.13 ± 0.19
6.7	−3.59	−3.82 ± 0.18
6.8	−3.31	−3.53 ± 0.17
6.9	−3.06	−3.27 ± 0.16
7.0	−2.82	−3.02 ± 0.15
7.1	−2.60	−2.79 ± 0.14
7.2	−2.40	−2.57 ± 0.14
7.3	−2.22	−2.38 ± 0.13
7.4	−2.05	−2.20 ± 0.13
7.5	−1.89	−2.04 ± 0.12
7.6	−1.75	−1.89 ± 0.12
7.7	−1.62	−1.75 ± 0.12
7.8	−1.50	−1.63 ± 0.11
7.9	−1.39	−1.51 ± 0.10
8.0	−1.29	−1.41 ± 0.10
8.1	−1.20	−1.31 ± 0.09
8.2	−1.12	−1.22 ± 0.09
8.3	−1.04	−1.13 ± 0.08
8.4	−0.97	−1.05 ± 0.08
8.5	−0.90	−0.98 ± 0.08
8.6	−0.83	−0.91 ± 0.07
8.7	−0.78	−0.84 ± 0.07
8.8	−0.72	−0.79 ± 0.07
8.9	−0.67	−0.74 ± 0.07
9.0	−0.63	−0.69 ± 0.07
9.1	−0.58	−0.65 ± 0.07
9.2	−0.55	−0.61 ± 0.07
9.3	−0.51	−0.57 ± 0.07
9.4	−0.48	−0.54 ± 0.07
9.5	−0.45	−0.51 ± 0.07

Our outermost energy $(-0.160\pm0.208)\times10^{-5}$ Ry at $R=15.0a_B$ was in good agreement with the accepted asymptotic result (-0.027×10^{-5} Ry, as found in BFL and references therein). Since the other theories are more accurate in this region, our energy was made equal to this value at this point. Through differencing, this had the effect of slightly raising the rest of the curve. This

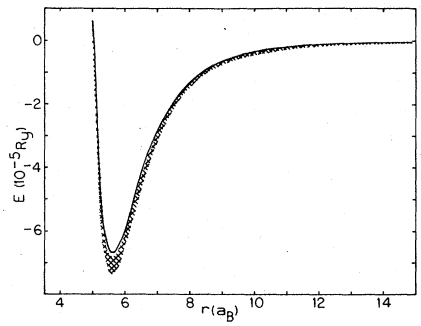

FIG. 1. Upper bound to the Born-Oppenheimer potential (hatched curve). The curve is two of our standard deviations wide. Solid line is the experimental curve of Burgmans, Farrar, and Lee.

also reduced the standard deviation in the fit to about equal to the standard deviation in the difference between these energies from the energy at $R = 15.0a_B$. Consequently, for the internuclear separations for which $E(R)$ was evaluated directly, the curve fit (Table IV) gives a better estimate to these energies than the direct calculations (Table III), since more information went into it.

Between these seven calculated energies there was error introduced by the looping of the fitting function. It was found that variation of the form of the fitting function and of the knot locations k_i produced variations in $E(R)$ between these points on the order of 0.3 standard deviations. The directly calculated points themselves, however, were independent of these variations (to within $0.1\sigma_{MC}$). The present fit was used because it looked smooth and had the qualitative features expected from the input.

NUMERICAL CHECKS

As long as the standard deviation (σ_{MC}) is accurate there are definite bounds on how far off the energy can be. This standard deviation [Eq. (12)] is a sum of squares, which makes it intrinsically easier to calculate accurately than the energy estimates. It was, in fact, this accuracy that enabled us to minimize the standard deviation over 1000 MC points. For $R = 5.6a_B$ this minimum σ_{MC} was 9.7×10^{-5} Ry or about the size of the well depth. As a check on these σ_{MC}'s, energies for partial runs were found to vary by the amount predicted from Eq. (12).

The standard deviations may, however, be artificially small if a region of the position space $\bar{x}$ is inadequately sampled. One way to be sure that this is not the case is to test the convergence property that σ_{MC} should have for large N. If all regions of the space are sampled enough this convergence is

$$\sigma_{MC} \propto 1/\sqrt{N}. \tag{19}$$

If, however, new Monte Carlo points are picked in previously inadequately sampled regions, then the standard deviation for a longer run will be larger than that predicted from Eq. (19). This is due to a small weight function w_i for these points appearing in the sums of Eq. (12). To check this, the standard deviations of various energies for ten partial runs with $N = 2000$ and 10 000 were compared to the average of ten partial runs with $N = 50\,000$. From the runs with $N = 2000$ and 10 000, the values predicted for $\sigma_{MC}(N = 50\,000)$ were equal to $\sigma_{MC}(N = 50\,000)$ to within uncertainties of 2% and 1%. In addition, it was possible to break the integration region into sections and sum the integrals over these to independently test whether each section was adequately sampled.

An integration by parts of the integral represented by Eq. (11) yields an integral which becomes

$$E_{Nt} = \frac{\sum_{i=1}^{N}[\Box\Psi_t(\bar{x}_i)\cdot\Box\Psi_t(\bar{x}_i) + V\Psi_t^2(\bar{x}_i)]/w_i}{\sum_{i=1}^{N}\Psi_t^2(\bar{x}_i)/w_i}, \tag{20}$$

where $\Box$ is the electronic gradient operator. As a check for coding errors this expression was evaluated concurrently with Eq. (11) over the same set of $\bar{x}_i$. To see the difference in Eq. (20) from Eq. (11), consider the kinetic-energy term for the simple atomic helium wave function

$$\Psi = e^{-2(r_1+r_2)}. \tag{21}$$

For Eq. (20) this is

$$\Box\Psi\cdot\Box\Psi = 8e^{-4(r_1+r_2)}, \tag{22}$$

with nothing to cancel the integrable singularities in the potential. The equivalent term for Eq. (11) is

$$-\Psi\Box^2\Psi = 4(1/r_1 + 1/r_2 - 2)e^{-4(r_1+r_2)}, \tag{23}$$

with the $4/r$ terms canceling with potential terms making $H\Psi/\Psi$ relatively constant. This, of course, makes Eq. (11) many times more precise using our methods than Eq. (21). Since these two equations are different and also weight differently the different regions of space, agreement between them is a good test for errors and for adequate sampling of the space of $\bar{x}$. These values from Eq. (20), are in agreement with the results from Eq. (11) (Table III) but with standard deviations on the order of 0.019 Ry. Energy differences can also be calculated using Eq. (20). This lowers the standard deviation to about 0.003 Ry—still in agreement with the much more accurate results from Eq. (11).

As a check on the weight functions and differencing technique, our first 80 000 MC points at $R = 6.6a_B$ were scaled to the system of two infinitely separated H_2 molecules. The relevant expression is

$$E_{H-H}=\tfrac{1}{2}\frac{\int\phi_{AB}(\vec{x}_1,\vec{x}_2)\phi_{CD}(\vec{x}_3,\vec{x}_4)H\phi_{AB}(\vec{x}_1,\vec{x}_2)\phi_{CD}(\vec{x}_3,\vec{x}_4)d\vec{x}_1d\vec{x}_2d\vec{x}_3d\vec{x}_4}{\int\phi^2_{AB}(\vec{x}_1,\vec{x}_2)\phi^2_{CD}(\vec{x}_3,\vec{x}_4)d\vec{x}_1d\vec{x}_2d\vec{x}_3d\vec{x}_4}, \tag{24}$$

where ϕ_{AB} is James and Coolidge's[20] 11-term trial H_2 wave function for electrons 1 and 2 on nuclei A and B, and H is the sum of the Hamiltonians for the two independent H_2 molecules:

$$H=H_{AB12}+H_{CD34}, \tag{25}$$

where

$$H_{AB12}=\nabla_1^2+\nabla_2^2-\frac{2}{r_{1A}}-\frac{2}{r_{1B}}-\frac{2}{r_{2A}}-\frac{2}{r_{2B}}+\frac{2}{r_{12}}+\frac{2}{r_{AB}}. \tag{26}$$

Note the absence of any cross-potential terms. The Monte Carlo estimate for this energy was

$$E_{MC}=\tfrac{1}{2}\frac{\sum_{i=1}^{80\,000}\frac{1}{w_i}(1+P_{23}+P_{24})\phi_{AB}(\vec{x}_{1i},\vec{x}_{2i})\phi_{CD}(\vec{x}_{3i},\vec{x}_{4i})(H_{AB12}+H_{CD34})\phi_{AB}(\vec{x}_{1i},\vec{x}_{2i})\phi_{CD}(\vec{x}_{3i},\vec{x}_{4i})}{\sum_{i=1}^{80\,000}\frac{1}{w_i}(1+P_{23}+P_{24})\phi^2_{AB}(\vec{x}_{1i},\vec{x}_{2i})\phi^2_{CD}(\vec{x}_{3i},\vec{x}_{4i})}, \tag{27}$$

where the x_i are electron positions originally picked with respect to the He-He system and then scaled to the $2H_2$ system using the method explained in Ref. 16; w_i is the weight function used to pick these original points multiplied by a scaling factor. The permutations were used to include all possible combinations with the same weight function and had the effect of reducing the standard deviation by smoothing the integral and by increasing the number of evaluations. At the nuclear separations ($R=r_{AB}=r_{CD}$) of 1.2, 1.4, 1.5, and $1.7a_B$ the energies were -4.416 ± 0.013, -4.674 ± 0.013, -4.612 ± 0.014, and -4.350 ± 0.010 eV compared with James and Coolidge's -4.41, -4.68, -4.63, and -4.35 eV.

CORRECTIONS

Since our trial wave functions are not exact eigenfunctions, the variational bounds would be above the correct eigenfunctions if the calculations were made over an infinite number of Monte Carlo evaluations. An estimate of the size of this effect can be made by assuming that this error is proportional to σ_M^2, the part of σ^2 which depends on nuclear separation distance $[\sigma^2=\sigma_M^2(R)+\sigma_A^2]$. During our search for the best wave function [lowest $\sigma_M^2(N=1000)$], energies were found for two of the earlier forms of the wave function at $R=5.6a_B$. A straight line fitted through the plot of E (-5.07 ± 0.60, -5.95 ± 0.41, $-0.716\pm0.33\times10^{-5}$ Ry) vs $\sigma_M^2(N=1000)$ (10.0, 1.8, 0.9×10^{-8} Ry^2) for these wave functions predicts that a perfect wave function $[\sigma_M^2(N=1000)=0]$ would have an energy lower than our present wave function by at most 0.18×10^{-5} Ry.

Kinetic energy estimates corresponding to the first term in Eq. (20) were summed concurrently with Eqs. (11) and (20). From these values (Table III), it is evident that our wave functions do not satisfy the virial theorem. This is not surprising since these wave functions were found by minimizing $\sigma^2(N=1000)$ rather than the energy. At the potential minimum, introducing a variational scaling parameter into the wave function and minimizing the energy with respect to this parameter[21] produces a new wave function which satisfies the virial theorem. The resulting bound for the scaled wave function is lower than that for the wave function at $R=5.6a_B$ in Tables I and II by 1.3×10^{-8} Ry.

Another correction, in comparing to the scattering experiments, is that due to our use of the Born-Oppenheimer approximation. These corrections have been examined by Laue,[22] who finds that the leading term which varies as R, is of the form of an expectation value of the interaction potential between the atoms divided by the nuclear masses. Since the expectation value is of the order of the dip in the Born-Oppenheimer potential, dividing by the nuclear masses makes this correction negligible.

CONCLUSION

At the potential minimum, our value is lower than the BFL result by 1.33σ. Since this is at the 82% confidence level, this curve should be considered in agreement with the BFL result with just a hint that the true curve is deeper than the BFL curve.

Finally, the standard deviations of the curve in Fig. 1 and Table IV are all smaller than the total electronic energy by factors less than 5.0×10^{-7}. This demonstrates that by using a combination of good weight-function techniques and very accurate wave functions, it is possible to get extremely accurate results from the Monte Carlo method.

ACKNOWLEDGMENTS

We would like to thank James Anderson for one very important conversation and A. A. Broyles for his support and helpful discussions. We also wish to thank Ron Schoenau and the rest of the University of Florida computing facility for their help in finding the hours of computing time required.

[1]L. W. Bruch and I. J. McGee, J. Chem. Phys. 52, 5884 (1970).
[2]H. G. Bennewitz, H. Busse, and H. D. Dohmann, Chem. Phys. Lett. 8, 235 (1970).
[3]J. M. Farrar and Y. T. Lee, J. Chem. Phys. 56, 5801 (1972).
[4]A. L. J. Burgmans, J. M. Farrar, and Y. T. Lee, J. Chem. Phys. 64, 1345 (1976).
[5]R. Chapman, Phys. Rev. A 12, 2333 (1975).
[6]J. C. Slater and J. G. Kirkwood, Phys. Rev. 37, 682 (1931).
[7]H. Margenau, Phys. Rev. 38, 747 (1931).
[8]D. R. McLaughlin and H. F. Schaefer III, Chem. Phys. Lett. 12, 244 (1971).
[9]P. Bertoncini and A. C. Wahl, Phys. Rev. Lett. 25, 991 (1970).
[10]B. Liu and A. D. McLean, J. Chem. Phys. 59, 4557 (1973).
[11]P. Bertoncini and A. C. Wahl, J. Chem. Phys. 58, 1259 (1973).
[12]P. D. Dacre, Chem. Phys. Lett. 50, 147 (1977).
[13]P. G. Burton, J. Chem. Phys. 70, 3112 (1979).
[14]G. Chalasinski and B. Jeziorski, Mol. Phys. 32, 81 (1976).
[15]Charles Schwartz, Phys. Rev. 128, 1146 (1962).
[16]R. L. Coldwell and R. E. Lowther, Int. J. Quantum Chem. Symp. 12, 329 (1978).
[17]R. L. Coldwell, Int. J. Quantum Chem. Symp. 11, 215 (1977).
[18]J. Kolwalik and M. R. Osborne, *Methods for Unconstrained Optimization Problems* (American Elsevier, New York, 1968).
[19]G. Starkschall and R. G. Gordon, J. Chem. Phys. 54, 663 (1971).
[20]H. M. James and A. S. Coolidge, J. Chem. Phys. 1, 825 (1933).
[21]B. L. Moisiewitsch, *Variational Principles* (Interscience, London, 1966).
[22]H. Laue, J. Chem. Phys. 46, 3034 (1967).